ICR The Institute of Cancer Research

Intensity Modulated High-Intensity Focused Ultrasound Treatment Planning

D. Sinden

Therapeutic Ultrasound, Division of Radiotherapy and Imaging, Institute of Cancer Research
david.sinden@icr.ac.uk

Therapy Ultrasound Interest Group Symposium, University of Oxford
July 1th 2013

Contents

"Immature poets imitate; mature poets steal; bad poets deface what they take, and good poets make it into something better, or at least something different."

T. S. Eliot, The Sacred Wood (1920)

Contents

Introduction
Similarities

Radiotherapy and ultrasound both propagate high frequency external beams which are beyond the detection of human senses.

Both are also used at low intensities for imaging and at higher intensities for therapeutic applications.

The Becquerel and Curie families were pioneers in the discovery and development of both ultrasound and then radiotherapy! Radiotherapy has far greater clinical acceptance and approved applications.

However, the different physical mechanisms of treatment leads to fundamentally different treatments protocols . . .

Introduction
Differences

Different physics

Radiotherapy	Acoustic
• light	• sound
• transverse wave	• longitudinal wave
• transport equations: linear	• KZK equation: nonlinear
• slight divergence	• convergent
• temporal fractionation	• spatial fractionation
• damage to DNA	• thermal ablation

Significant difference is the size of the volume which can be exposed: radiotherapy can treat large volumes, where as a single lesion in HIFU is typically smaller. Thus breathing motion is significant for the placement of single lesion.

Volumetric modulated arc therapy

Volumetric modulated arc therapy (VMAT) is the hot topic in radiotherapy

VMAT delivers radiation by rotating the gantry of a linear accelerator through one or more arcs with the radiation continuously on. It varies:

(i) the multi-leaf collimator (MLC) aperture shape
(ii) the MLC orientation
(iii) the fluence-output rate
(iv) the gantry rotation speed

Origin of the method begins with intensity-modulated arc therapy[1]

[1] C. X. Yu "Intensity-modulated arc therapy with dynamic multileaf collimation: an alternative to tomotherapy" *Phys. Med. Biol.* **40** (1995) pg. 1435–1450.

Volumetric modulated arc therapy

Figure: Rotating gantry and treatment head. Image courtesy of Elekta AB.

Contents

Discretisation 1

Define

- Gross tumour volume (visible tumour)
- Clinical treatment volume (GTV + uncertainty)
- Planned treatment volume (CTV +resection margin)

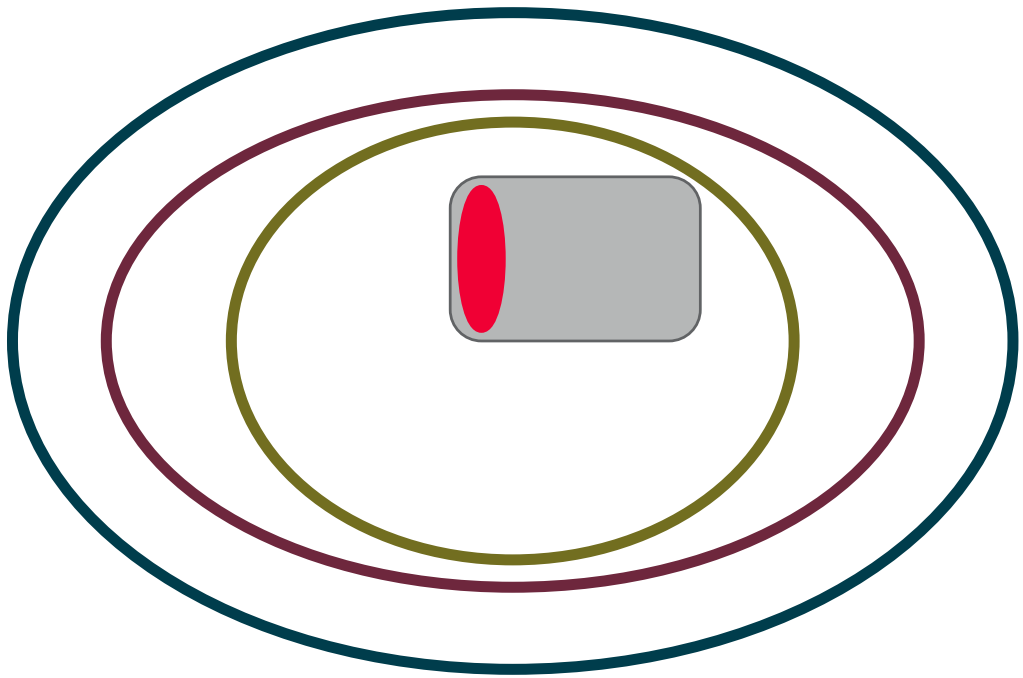

Treatment shot

Check region

Is the planned treatment volume equal to the clinical treatment volume?

Discretisation 2

Define check regions (boxes) and transducer settings (coloured) for each region, based on depth, tissue properties, vasculature etc

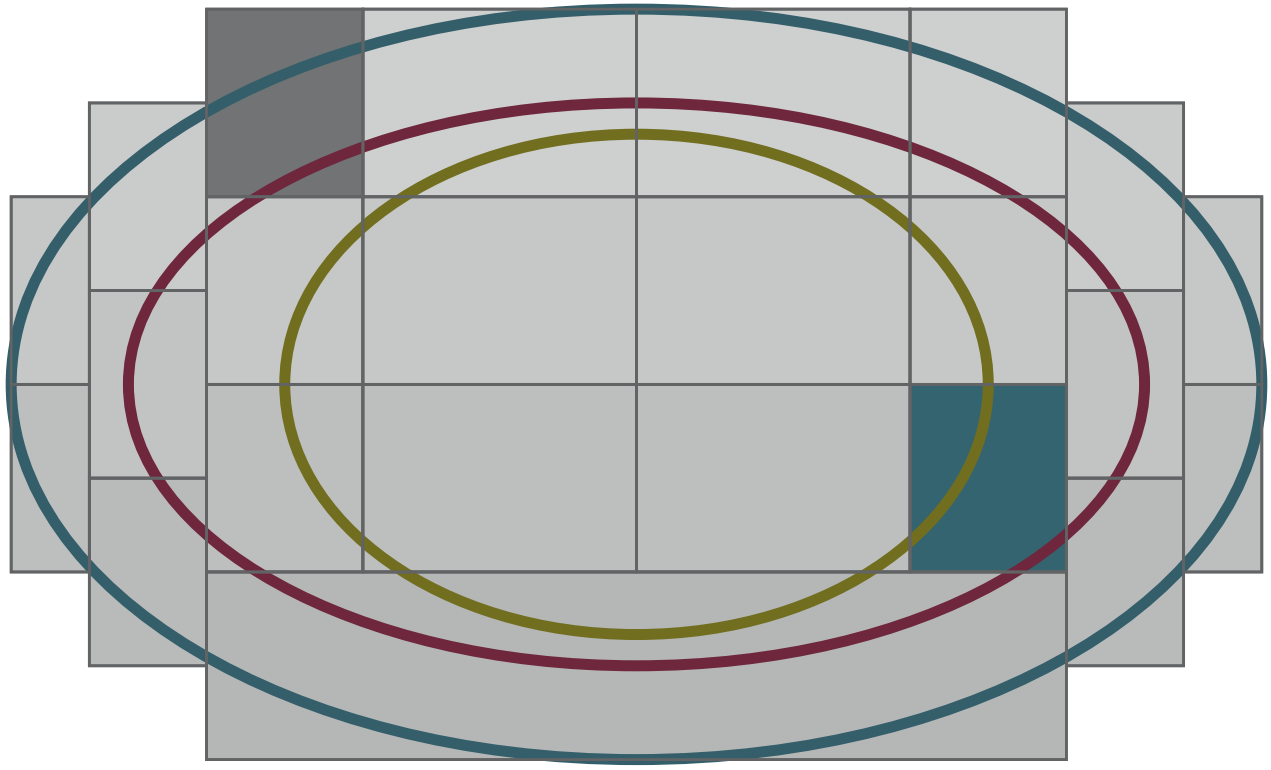

Transcostal treatment

For potential transcostal treatment motion is due to respiratory cycle.

As liver is attached to the diaphragm by areolar tissue and the coronal ligaments the upper part of the liver, and as such experiences significant deformation in the coronal plane during the breathing cycle.

Displacement in other planes is an order of magnitude less. [1]

[1] F. Marquet et al. "Optimal transcostal high-intensity focused ultrasound with combined real-time 3D movement tracking and correction" *Phys. Med. Bio.* **56** (2011) pg. 7061–7080

Displacement

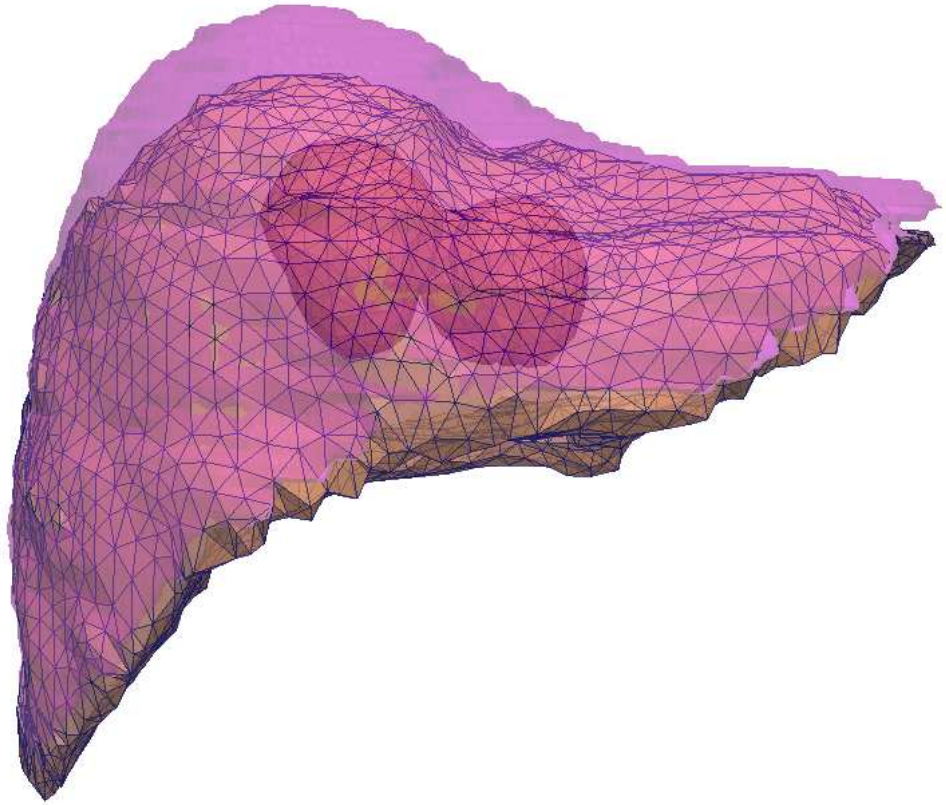

Figure: Liver motion meshed at both maximum and minimum displacements from exhalation baseline. Image courtesy of Lianghao Han (UCL, CMIC)

Displacement

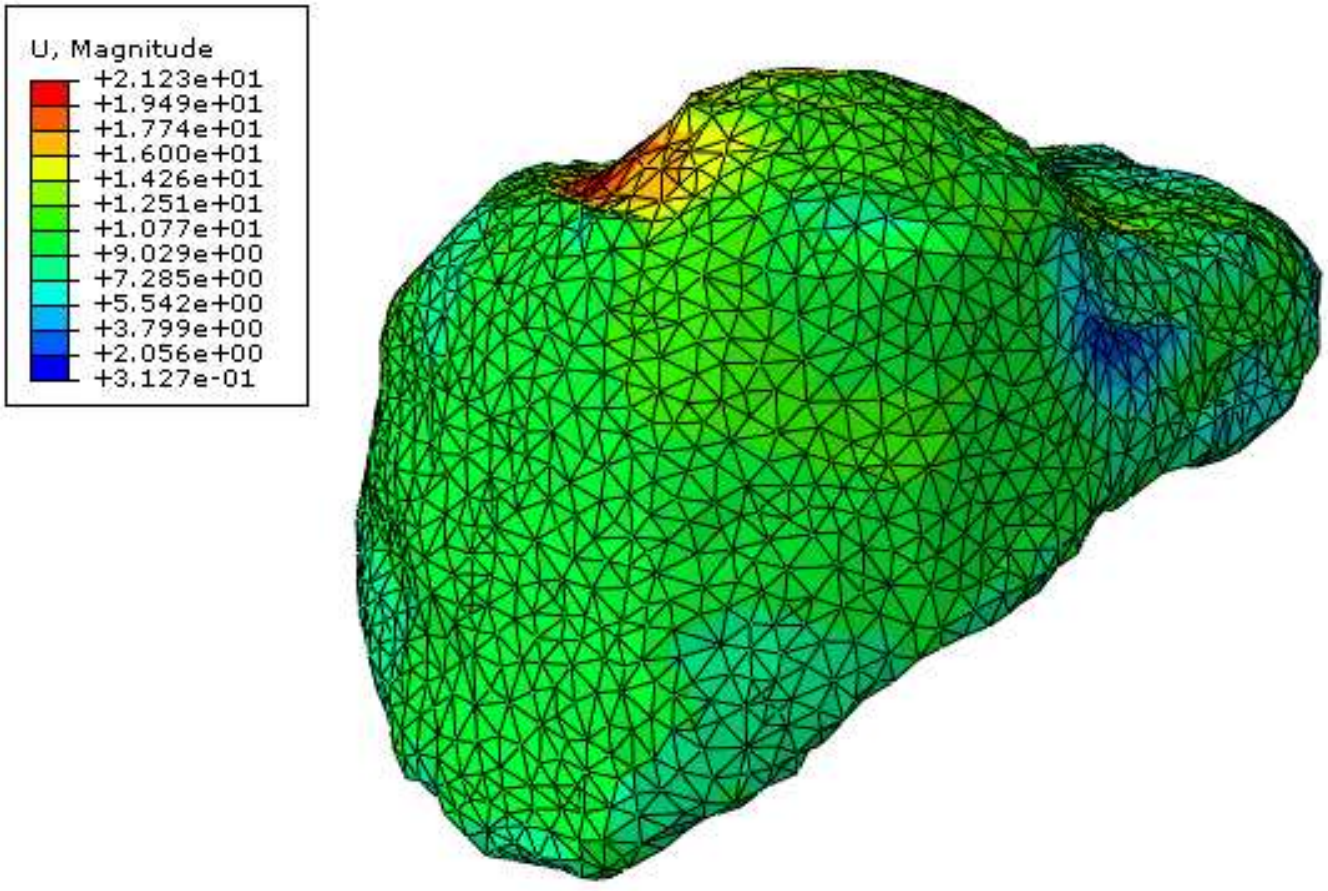

Figure: Liver motion scaled according to maximum displacement (mm). Image courtesy of Lianghao Han (UCL, CMIC)

Displacement

- Key physical property is that the motion in the axial plane is small compared to transverse planes. Furthermore motion of ribs is also small compared to motion in coronal plane.
  - $\Rightarrow$ Assume that, in the absence of the ribs shielding the target, the acoustic field is approximately constant throughout the exposure duration.

That is, assume the target moves and the acoustic field remains fixed.

Motion Compensation

Phased arrays 1

Electronic steering of the focus has been proposed as a means of tracking the moving target. However electronic steering results in a loss of intensity. Also latency in steering may pose a problem in delivering real-time adaptive focusing.

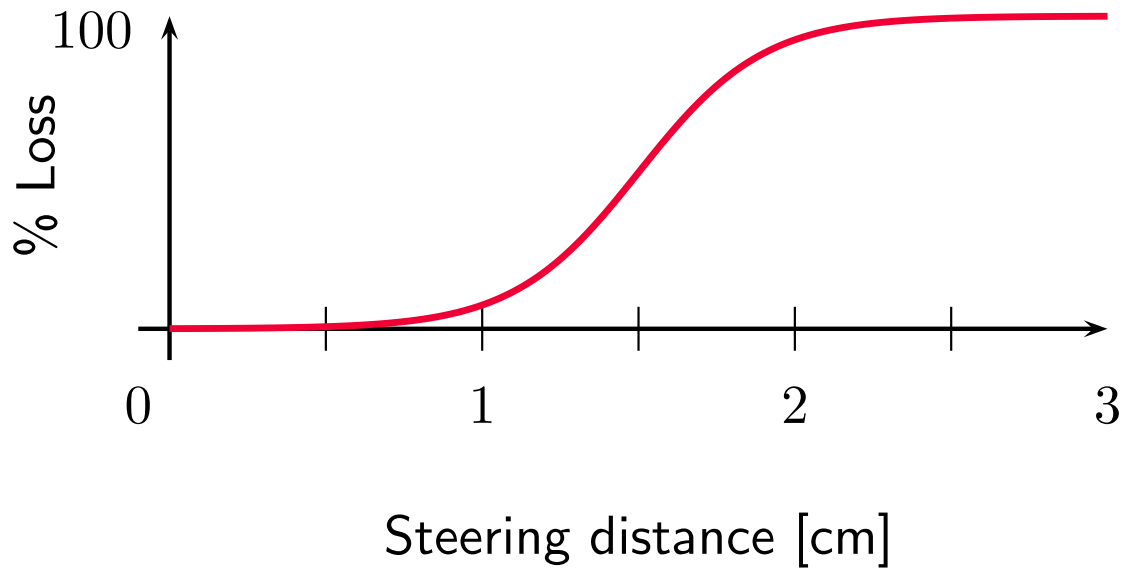

Motion Compensation
Phased arrays 2

A discrete approximation to tracking the breathing cycle may be implemented.

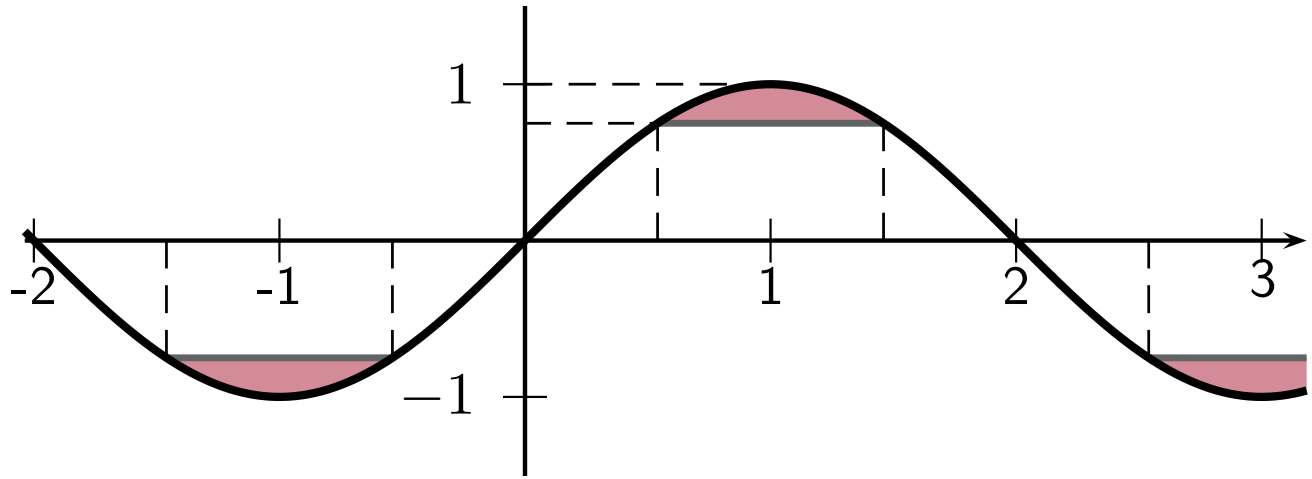

The acoustic window can control the volume ablated.

Motion Compensation or Exploitation?

A motion compensation model may simply ‘gate’ the firing of the beam to the hit the intended location.

Why? Simply allow the breathing motion to move the relative position of the focus: motion will lead to a larger volume being exposed and may result in a larger volume being treated.

But how will this affect the volume and shape of the lesion?

Beside changing the relative velocity of the target, potentially the same control parameters as VMAT are available

Contents

Objectives Functions

From a treatment planning perspective what is the intended dose? Two primary measures

- A Cumulative Equivalent Minutes formulation, i.e. CEM_{240}

or

- Maximum temperature

For either measure, a useful tool is the marching cubes algorithm for extracting a surface from a volume. From an accurate extracted surface mesh, and the computation of the outward facing normal vectors, Gauss's second identity can be used to compute the volume enclosed.

Without Gating

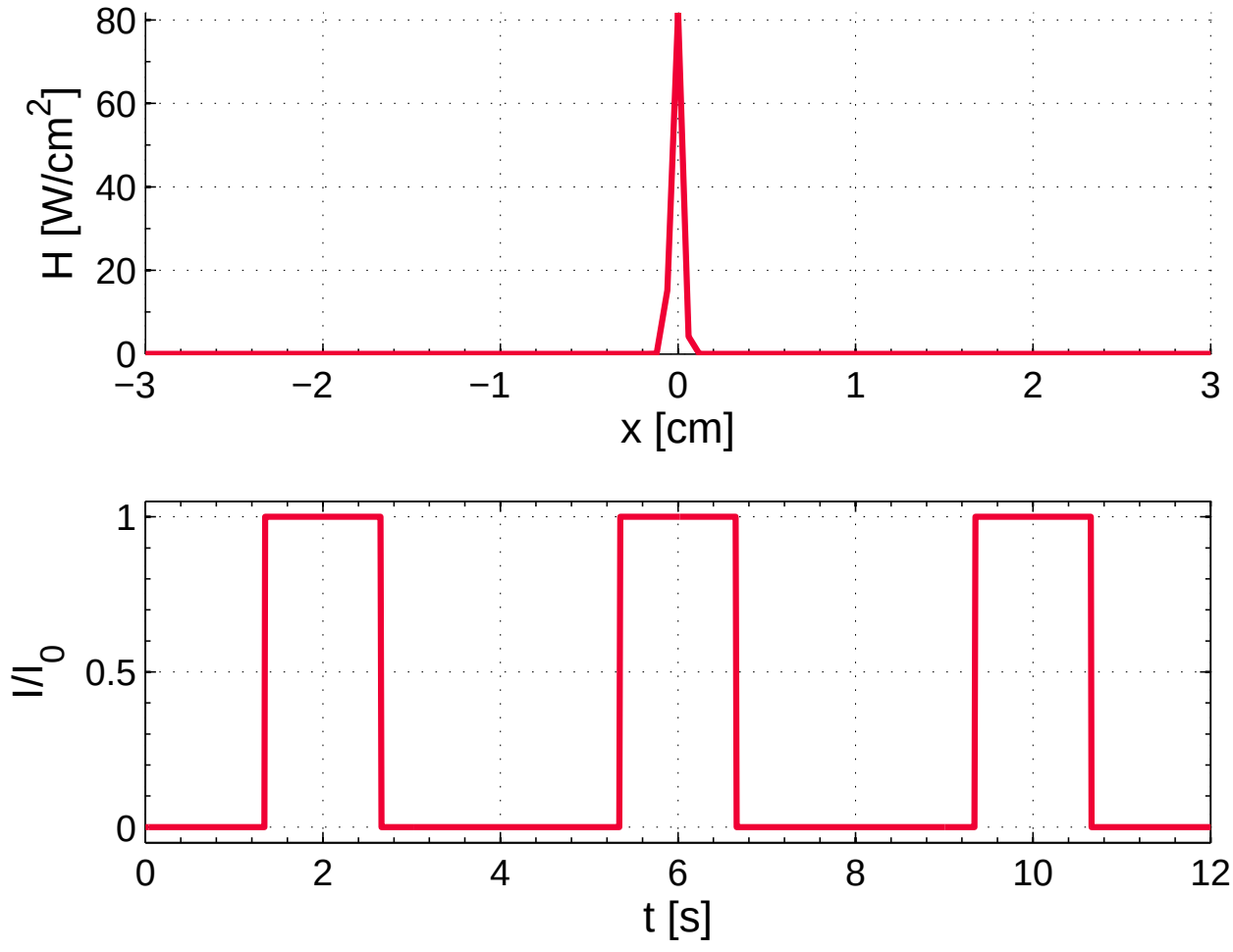

Figure: The spatial profile of the heating rate used in the bioheat equation and the triggering sequence.

Without Gating

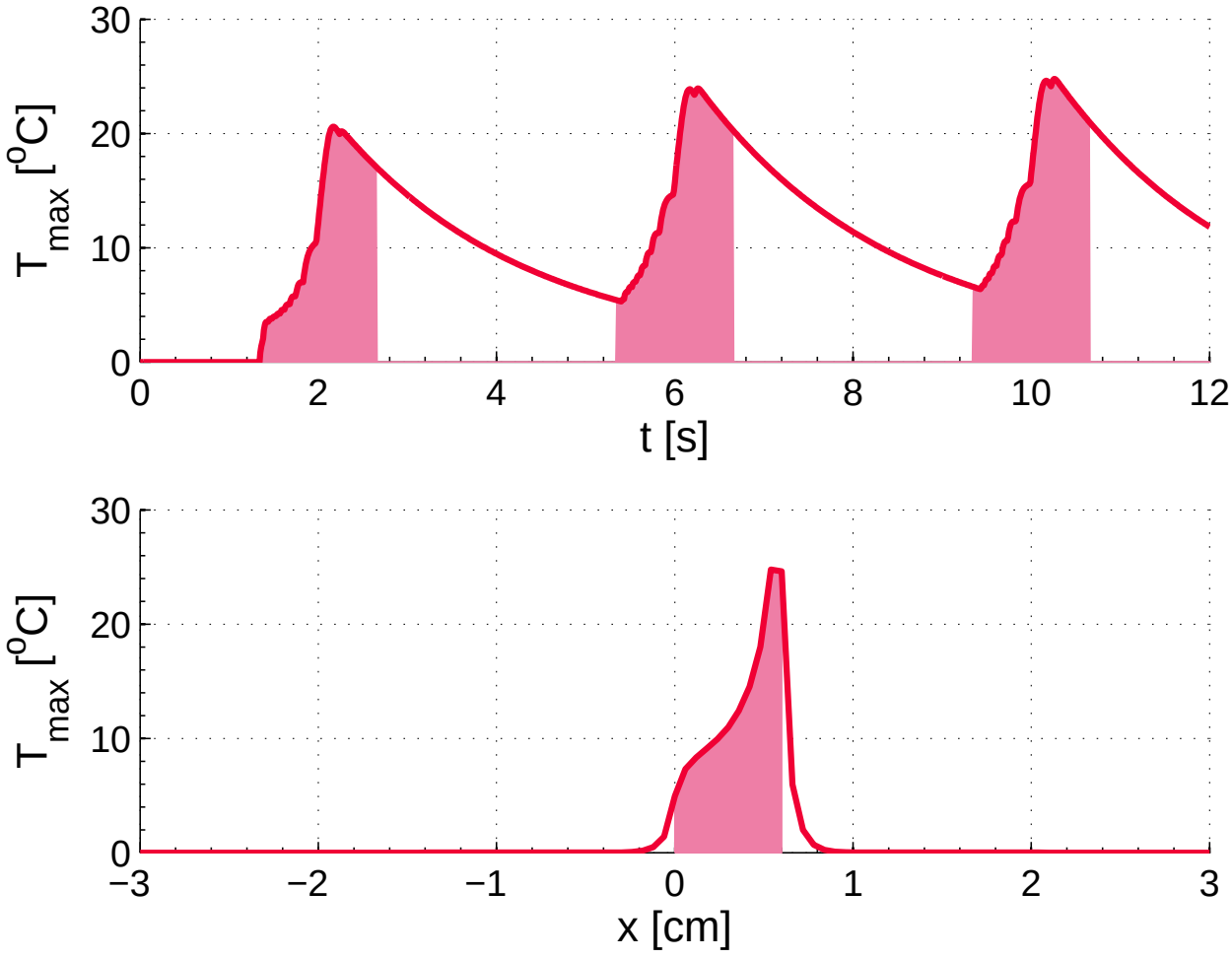

Figure: The maximum temperatures within the target volume as a function of time and space. The shaded regions denote the times and position which were exposed to ultrasound. Note that the maximum temperature achieved does not occur at the end of the exposure!

Without Gating

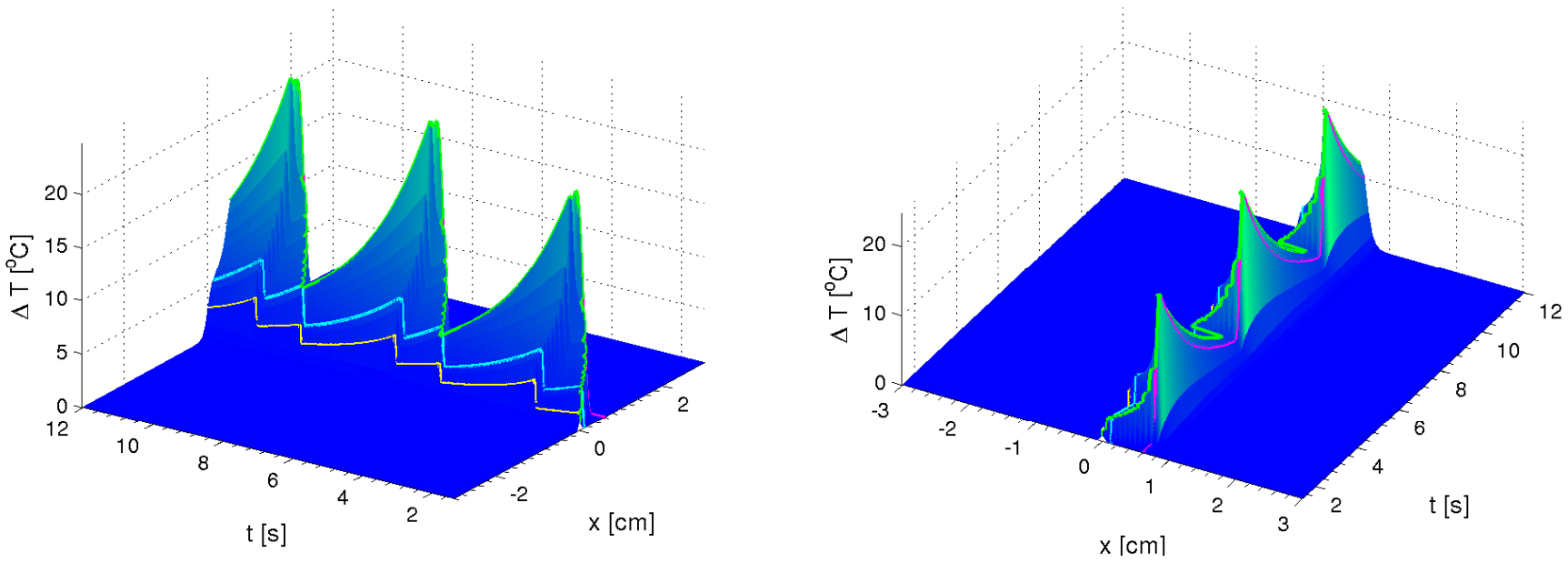

Figure: 'Hybrid images' of one-dimensional spatial and temporal thermal surface, in which the thermal profiles from different positions in the target volume are illustrated. Note that the contrast between those position which lie at the start and peak of the breathing cycle in terms of the shape of the profiles and the number of distinct peaks.

Without Gating

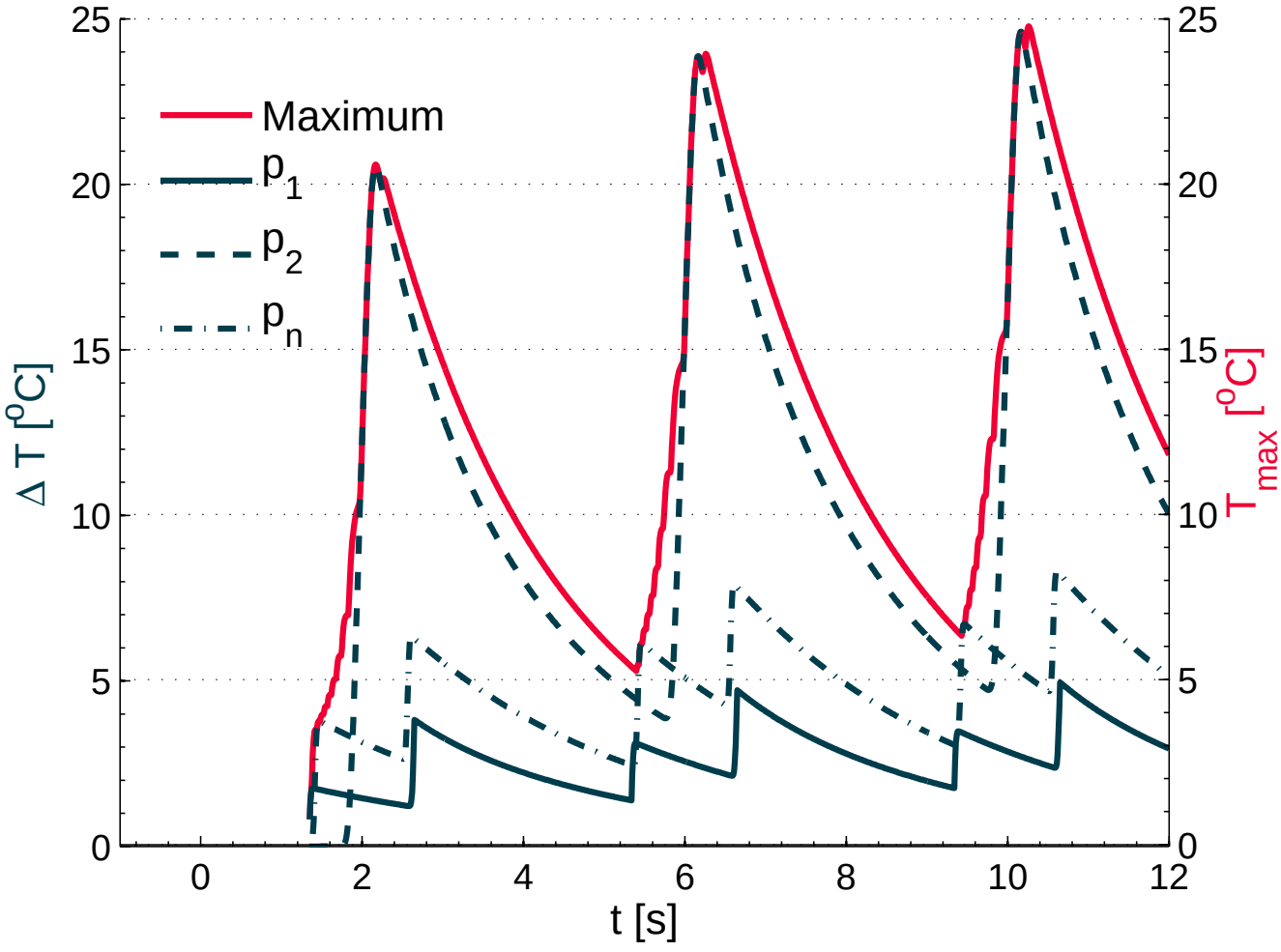

Figure: Thermal profiles of a number of points within the region exposed to ultrasound, as well as the maximum temperature throughout the exposure. In this figure p_1 is the point which is first exposed, p_n the point which is last exposed.

Without Gating

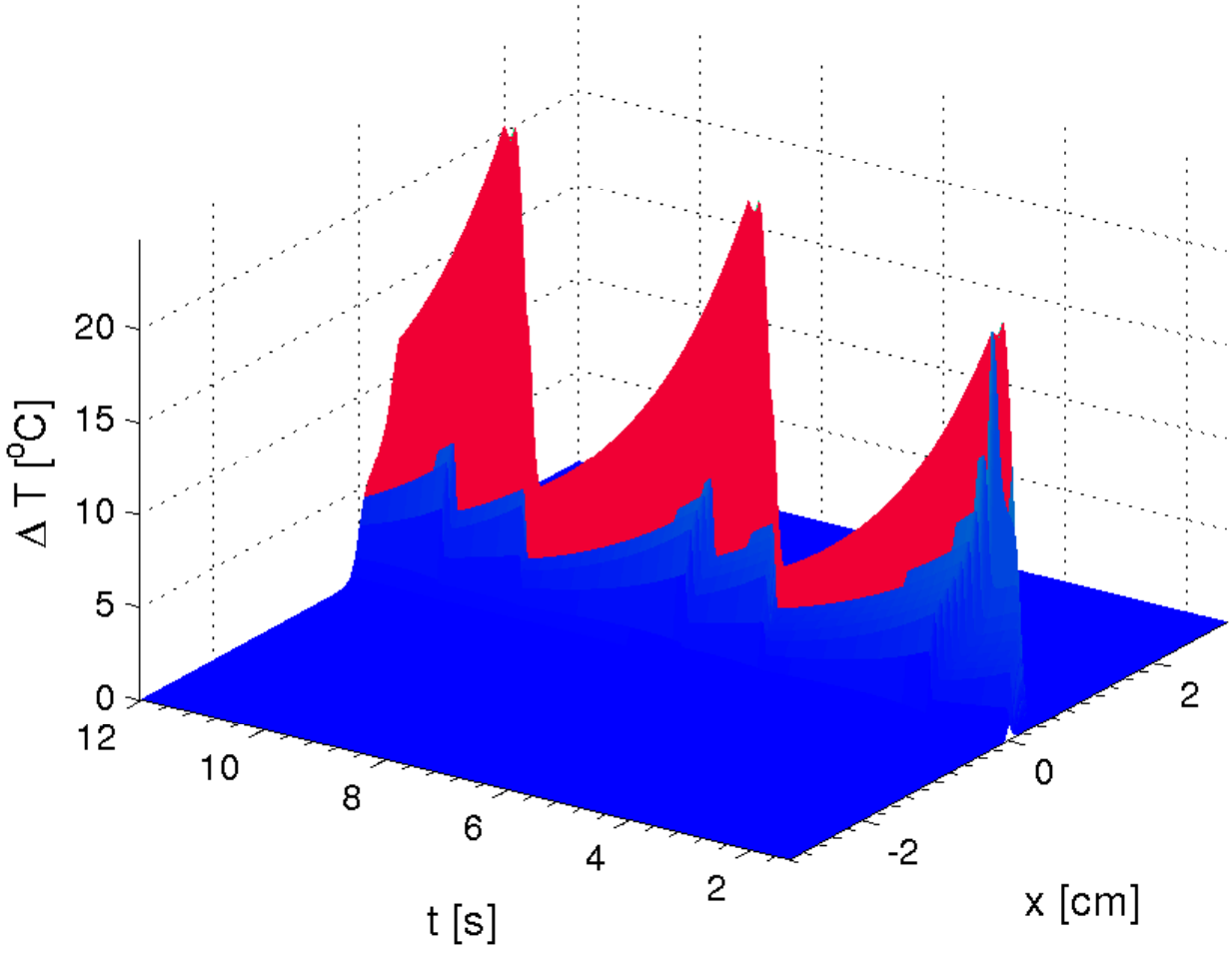

Figure: 'Hybrid image' of one-dimensional spatial and temporal thermal surface, in which regions which are classified as being treated according to the cumulative equivalent minutes formulation are coloured in red.

Without Gating

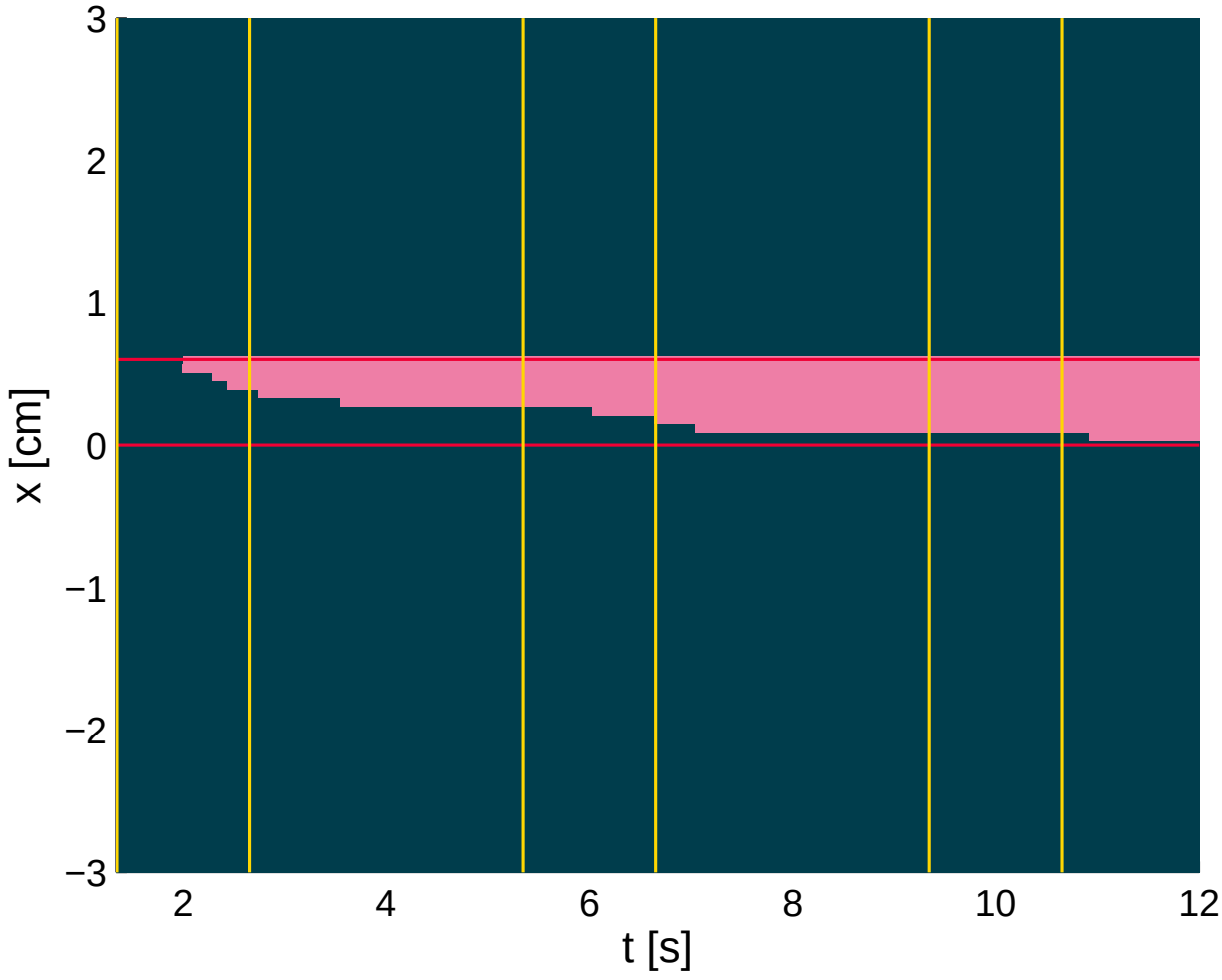

Figure: Planar representation of binary ‘map’ of treated regions. The boundaries of the one-dimensional region exposed to ultrasound are also illustrated.

Alternating-Direction-Implicit Schemes

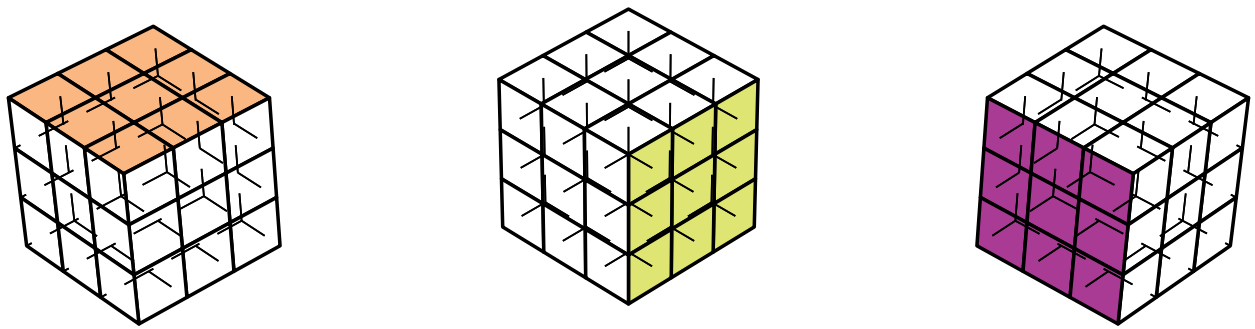

Split one three-dimensional problem up into three one-dimensional problems which can be solved easily.[1]

[1] J. Douglas and J. E. Gunn, "A general formulation of alternating direction methods," *Numerische Mathematik* **6**, (1964) pg. 428–453.

Numerical Scheme

Pennes bioheat equation

$$\rho C \frac{\partial T}{\partial t} = \kappa \nabla^2 T + \omega_p \left(T - T_\infty\right) + h\left(\boldsymbol{x}, t\right)$$
$$= \kappa \left(\frac{\partial^2 T}{\partial x^2} + \frac{\partial^2 T}{\partial y^2} + \frac{\partial^2 T}{\partial z^2} \right) + \omega_p \left(T - T_\infty\right) + h\left(\boldsymbol{x}, t\right)$$

where ρ is the density, C is the specific heat, κ is the thermal conductivity, ω_p is the bulk perfusion rate, T_∞ is the ambient temperature and h is the heating rate.

Numerical Scheme

Discretise T_i^n and let $f(T) = \kappa \nabla^2 T + \omega_p \left(T - T_\infty\right) + h\left(\boldsymbol{x}, t\right)$, and $A_x = \dfrac{\kappa}{\rho C} \dfrac{\Delta t}{\Delta x^2} \delta_x$, where δ_x is the central difference approximation of the second order partial derivative, and $g = \omega_p \left(T - T_\infty\right) + h\left(\boldsymbol{x}, t\right)$.

First apply a Crank-Nicolson scheme:

$$\frac{T_i^{n+1} - T_i^n}{\Delta t} = \frac{f(T^{n+1}) + f(T^n)}{2}$$

and seek to find the solution for T^{n+1}.

Numerical Scheme

Now introducing three intermediate time-steps and deforming the operator

$$\left(1-\frac{A_x}{2}\right)T^{n+1/3} = \left(1+\frac{A_x}{2}+A_y+A_z\right)T^n + \Delta t G^n$$

$$\left(1-\frac{A_y}{2}\right)T^{n+2/3} = \left(1+\frac{A_x}{2}+\frac{A_y}{2}+A_z\right)T^n + \frac{A_x}{2}T^{n+1/3}$$

$$\left(1-\frac{A_z}{2}\right)T^{n+1} = \left(1+\frac{A_x}{2}+\frac{A_y}{2}+\frac{A_z}{2}\right)T^n + \frac{A_x}{2}T^{n+1/3} + \frac{A_y}{2}T^{n+2/3} + \frac{\Delta t}{2}\left(G^{n+1}-G^n\right)$$

So that the factorised system, after discarding small terms is the same as the original system

Numerical Scheme

The operator splitting models the system

$$\left(1-\frac{A_x}{2}\right)\left(1-\frac{A_y}{2}\right)\left(1-\frac{A_z}{2}\right)T^{n+1} = \left(\left(1+\frac{A_x}{2}\right)\left(1+\frac{A_y}{2}\right)\left(1+\frac{A_z}{2}\right)-\frac{A_xA_yA_z}{4}\right)T^n + \frac{\Delta t}{2}\left(G^n+G^{n+1}\right)-\frac{\Delta t}{2}\left(A_x+A_y-\frac{A_xA_y}{2}\right)\left(G^{n+1}-G^n\right)$$

which is a good approximation to the bioheat equation.

Thermal History

The scheme can easily be extended to include temperature dependent changes in material properties[1].

$$\begin{aligned}\frac{\partial T}{\partial t} &= \nabla \cdot (\kappa(T)\nabla T) + \omega_p \left(T - T_\infty\right) + h\left(\boldsymbol{x}, t\right) \\ &= \kappa \nabla^2 T + \kappa' \left(\nabla T\right)^2 + \omega_p \left(T - T_\infty\right) + h\left(\boldsymbol{x}, t\right)\end{aligned}$$

So the governing equation is a quasi-linear equation, but a corresponding operator A_x can still be defined, but more intermediate time-steps are required.

---

1 A. Bhattacharya and R. L. Mahajan "Temperature dependence of thermal conductivity of biological tissues" *Physiol. Meas.* **24**(3) (2003) pg. 769–784.

Numerical Scheme

Assume that the heat is localised and that the size of the computation domain is sufficiently large to apply Dirichlet boundary conditions. Thus the matrix to be inverted is tridiagonal and hence can be solved in $\mathcal{O}(n)$ steps.

The primary advantage is the method parallelises very easily on high-performance computing systems, especially on shared memory systems. Essentially, for each one-dimensional step, the domain can be truncated into as many cores are available.

Truncation error $\varepsilon = \mathcal{O}(\Delta t^2) + \mathcal{O}(\Delta x^2) + \mathcal{O}(\Delta y^2) + \mathcal{O}(\Delta z^2)$

Unconditionally stable.

Contents

Optimization

The idea of intensity modulated HIFU is to discretely vary the applied intensity to conform the dose distribution within each enlarged subvolume to an intended size or shape.

- The time period which the ultrasound is exposed to the target is discretised into an number of intervals. In each interval the heating rate can be specified within some interval. These are the control parameters.
- A cost function $\Omega = \sum_i \Omega_i$ is defined over some portion of the target area.
- The optimisation scheme attempts to choose the best values of the intensities within each time interval so that the cost function is minimized.

Optimization

Many optimisation schemes require a measure of how the cost function changes as the control parameters are changed: the computation of the Jacobian can be computationally demanding and is the reason a rapid numerical method is employed.

$$J = \begin{pmatrix} \frac{\partial \Omega_1}{\partial p_1} & \frac{\partial \Omega_2}{\partial p_1} & \cdots & \frac{\partial \Omega_n}{\partial p_1} \\ \frac{\partial \Omega_1}{\partial p_2} & & & \\ \vdots & & & \\ \frac{\partial \Omega_1}{\partial p_m} & & & \end{pmatrix}$$

Constraints

Some bound constraints need to be applied to the control parameters which

- limit the possible power output to physically admissible values

and also

- enforce that the heating rate is non-negative (or strictly positive)

in order to get physically meaningful results!

Efficiency

The code (at roughly `1,500` lines long) was:

- written in `fortran`,
- compiled with the Intel `ifort` compiler

and

- uses the Intel `mkl` packages with reverse communication interface to handle matrix-vector multiplication and preconditioning at separate stages. Jacobian is computed.

On the ICR cluster: in both serial and parallel single subvolume simulations of a 12 second exposure 36cm^3, discretised with $\Delta t = 0.1$s and $\Delta x = 0.5$cm can take less than 30 seconds to run.

Optimization

Care is needed as typically there is always a solution which the algorithm can converge to!

For example, if the maximum temperature at every the control points is equal to the average, i.e. a top hat function, then this simply means that the zero solution is the preferred solution. A lower bound constraint becomes the next best solution, which may satisfy the tolerances imposed.

Contents

Results

Simple to ensure a maximum temperature at a point by the optimization scheme: potential use in lesioning thresholds

Results

Preliminarily results: attempt to ensure symmetric dose about the unoptimized peak or around the mid point.

Control parameters varied between 5 intervals in each breathing cycle, so 15 modulations

As on going work tolerances not too great

Results

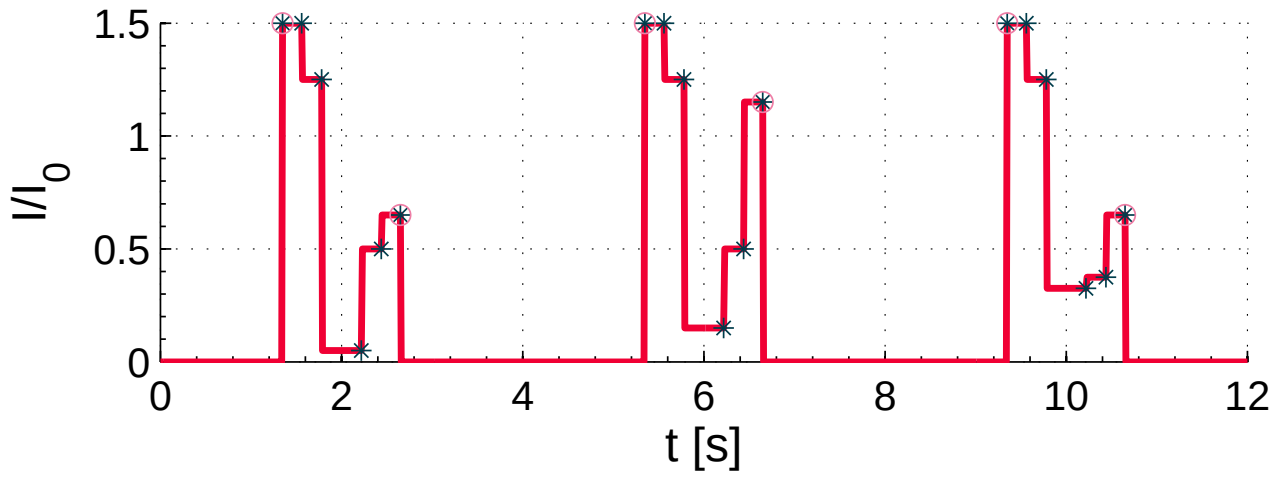

Figure: Modulated intensities

Results

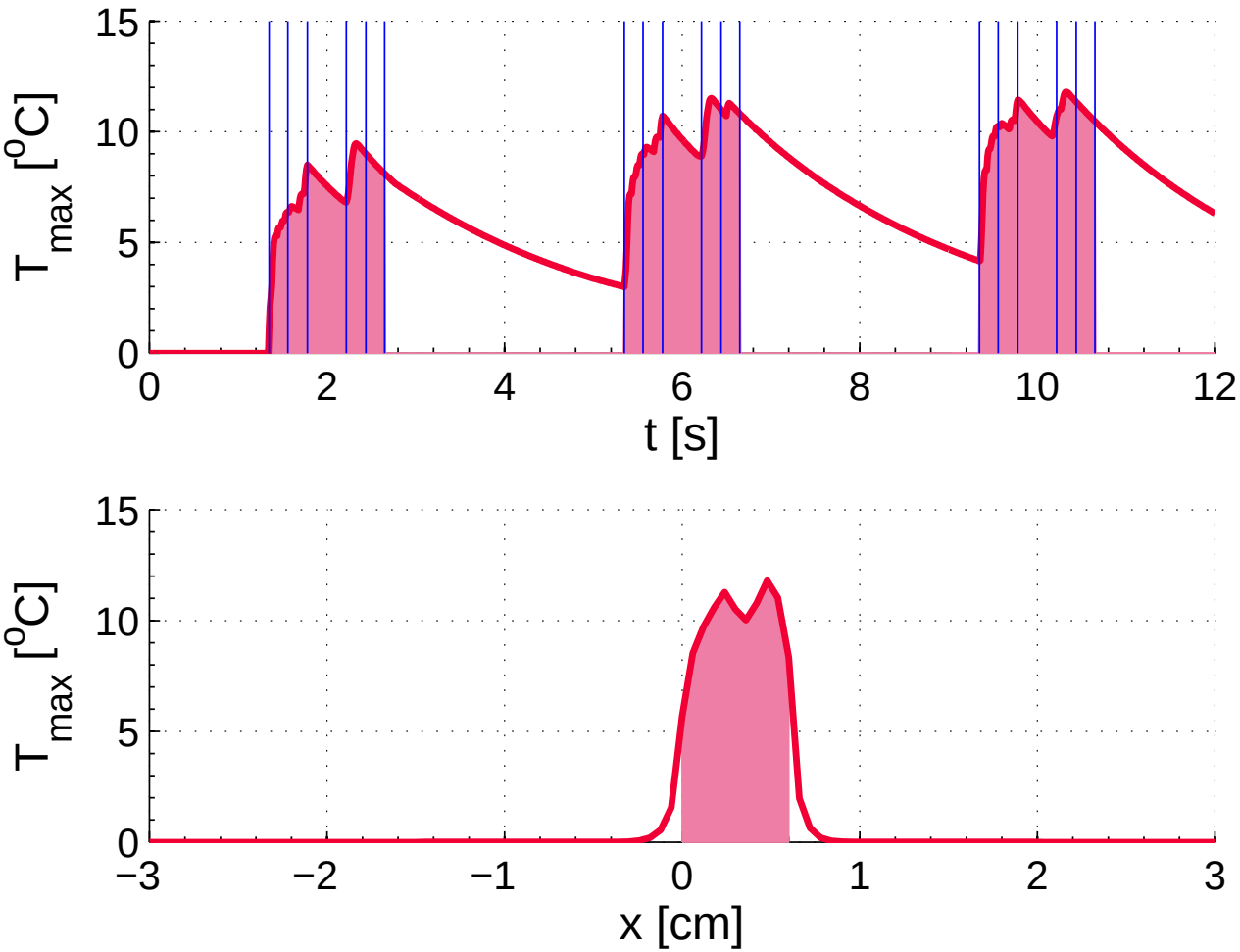

Figure: Maximum temperatures as a function of time and space from modulated intensities.

Results

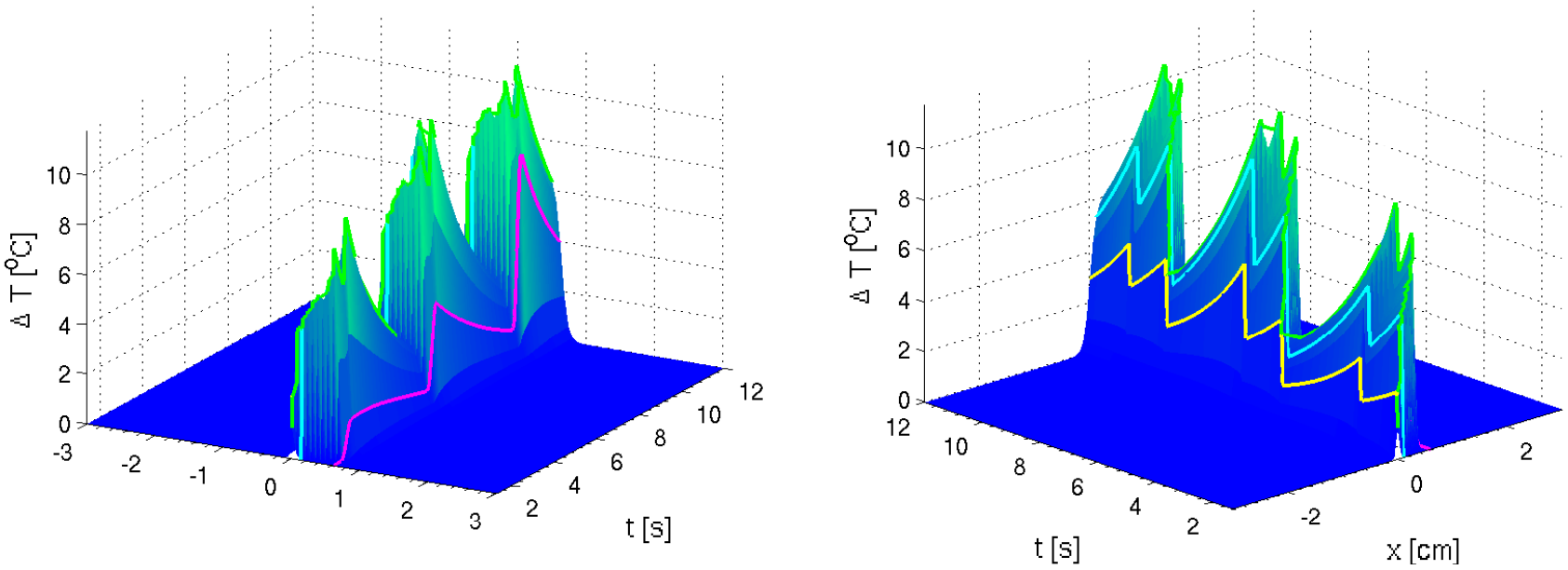

Figure: 'Hybrid images' of one-dimensional spatial and temporal thermal surface, in which the thermal profiles from different positions in the target volume are illustrated. Note that the contrast between those position which lie at the start and peak of the breathing cycle in terms of the shape of the profiles and the number of distinct peaks.

Results

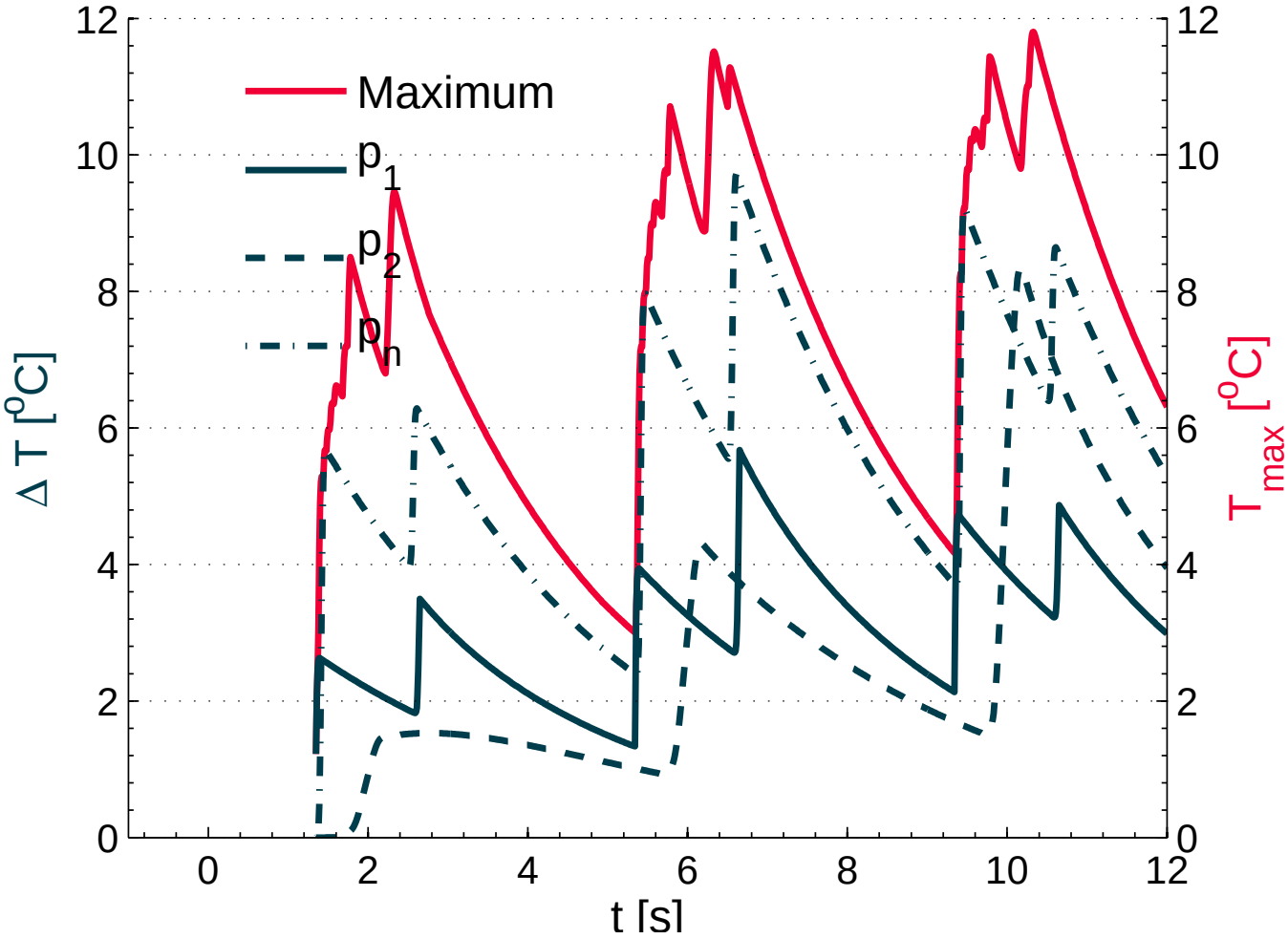

Figure: Thermal profiles of a number of points within the region exposed to ultrasound, as well as the maximum temperature throughout the exposure. In this figure p_1 is the point which is first exposed, p_n the point which is last exposed.

Contents

Conclusions

- Rapid and robust numerical solver developed, capable of running on desktop or cluster.
- Proof of concept demonstrated : intensity modulated high-intensity ultrasound can be used, for some cost functions, to provide a more symmetric distribution of maximum temperature dose.
- Procedure established to enlarge subvolumes and potentially reduce treatment times.
- Still a work in progress!

Future Work

- Further investigation of different cost functions and control points
- Displacement in three planes
- Different, realistic, breathing motion
- Experimental validation in phantoms and *in vivo*
- Smooth variation in intensity with time based on control points

Observation

Motion compensation:

- reduces the spatial peak intensity and maximum temperature in comparison with continuous, static exposures

and

- increases the full-width half maximum of the temperature distribution in the principal direction of motion.

In the principal direction of motion the ‘effective frequency’ is reduced.

Open Question

An inverse problem:

what shape transducer would give a focal volume with three different full-width half maxima?

Typically the diameter and radius of curvature determine the two principal axes (σ_r, σ_z) of the full width half maxima, now a third variable is required: either a second radius of curvature or diameter ...

Transcostal High-Intensity Focussed Ultrasound for the Treatment of Cancer

UCL: Nader Saffari, Pierre Gélat, Gregory Vilensky, David Hawkes, Dean Barratt, Daniel Heanes, Lianghao Han.

ICR: Gail ter Haar, Ian Rivens, Lise Retat, Richard Symonds-Tayler, John Civale.

BUBL: Constantin Coussios, Stéphane Labouret, David Holroyd, Eleanor Stride.

Oxford: David Cranston, Tom Leslie.

Consultants: David Cosgrove, Ivan Graham.

EPSRC: For financial support under

- EP/F025750/1
- EP/F02617X/1
- EP/F029217/1

Thank you for your attention
Any questions?